Carbohydrate Polymers 97 (2013) 1–8

Contents lists available at SciVerse ScienceDirect

Carbohydrate Polymers

journal homepage: www.elsevier.com/locate/carbpol

Nano-structure of heat–moisture treated waxy and normal starches

Wittawat Jiranuntakul[a], Shigeru Sugiyama[b], Kazumi Tsukamoto[b], Chureerat Puttanlek[c], Vilai Rungsardthong[d], Santhanee Puncha-arnon[a], Dudsadee Uttapap[a,*]

[a] Division of Biochemical Technology, School of Bioresources and Technology, King Mongkut's University of Technology Thonburi, 49 Soi Tientalay 25, Bangkhuntien-Chaitalay Road, Takham, Bangkhuntien, Bangkok 10150, Thailand
[b] Nanobiotechnology Laboratory, National Food Research Institute, National Agriculture and Food Research Organization, 2-1-12, Kan-nondai, Tsukuba 305-8642, Japan
[c] Department of Biotechnology, Faculty of Engineering and Industrial Technology, Silpakorn University, Nakorn Pathom 73000, Thailand
[d] Department of Agro-Industrial Technology, Faculty of Applied Science, King Mongkut's Institute of Technology North Bangkok, 1518 Pibulsongkram Road, Bangsue, Bangkok 10800, Thailand

ARTICLE INFO

Article history:
Received 24 August 2012
Received in revised form
23 November 2012
Accepted 12 April 2013
Available online 24 April 2013

Keywords:
Heat–moisture treatment
Atomic force microscopy
Nano-structure
Normal starch
Waxy starch

ABSTRACT

Surface regions of untreated and heat–moisture treated (HMT) normal rice, waxy rice, normal corn, waxy corn, normal potato, and waxy potato starch granules were examined by atomic force microscopy (AFM). AFM images revealed surface roughness of untreated starch granules and protrusions with a diameter of approximately 15–90 nm. After treatment, the smooth surface region on starch granules was observed, especially in normal rice, waxy rice, and normal corn starches. A significant reduction in the size of protrusions on the surface of HMT potato starch granules was also detected. The newly formed structures may act as barriers and retard water penetration into starch granules. The blocklet model of starch granule architecture was also confirmed by the AFM images.

1. Introduction

Heat–moisture treatment (HMT) refers to a physical modification of starch through incubation of starch granules at low moisture levels, below 35%, and heating at high temperature, above the glass transition temperature but below the gelatinization temperature, during a certain period of time (Jacobs & Delcour, 1998). Numerous studies have demonstrated the effects of such treatments on the structure and physicochemical properties of cereal, tuber, and legume starches, including significant changes in X-ray diffraction pattern, crystallinity, granule swelling, amylose leaching, viscosity, gelatinization parameters, retrogradation, and acid/enzyme susceptibility (Chung, Hoover, & Liu, 2009; Hoover & Manuel, 1996; Hormdok & Noomhorm, 2007; Jiranuntakul, Puttanlek, Rungsardthong, Puncha-arnon, & Uttapap, 2011; Juansang, Puttanlek, Rungsardthong, Puncha-Arnon, & Uttapap, 2012; Shih, King, Daigle, An, & Ali, 2007; Singh, Bawa, Riar, & Saxena, 2009; Varatharajan, Hoover, Liu, & Seetharaman, 2010; Vieira & Sarmento, 2008; Watcharatewinkul, Puttanlek, Rungsardthong, & Uttapap, 2009; Watcharatewinkul, Uttapap, Puttanlek, & Rungsardthong, 2010; Zavareze, Storck, Castro, Schirmer, & Dias, 2010). Possible explanations for the observed effects of HMT on starch properties were gathered by Jacobs and Delcour (1998). These included: (1) changes with respect to crystallinity – either a change in the packing arrangement of double helices in starch crystallites from B- to A-type crystallinity, or development of new crystallites in the amorphous regions (formation of amylose crystallites or formation of crystalline amylose–lipid complexes); (2) changes with respect to the amorphous fraction (increase in order, without increase in crystallinity) such as increased interactions between amylose chains or between amylose and amylopectin, extra formation of amylose–lipid complexes, or transformation of amorphous amylose into a helix; and (3) alterations of the interactions between crystallites and the amorphous parts. Besides these, other changes at the molecular, nano- or microstructural level, which have not yet been identified, might also be involved in the physicochemical changes of starch after HMT.

Our previous reports have described the microstructure, physicochemical properties and molecular structure of waxy and normal rice, corn, and potato starches modified by HMT at 100 °C for 16 h with starch moisture content of 25%. Scanning electron micrographs showed that HMT did not change the size, shape or surface characteristics of corn and potato starch granules, while

* Corresponding author. Tel.: +66 2470 7754; fax: +66 2452 3479.
E-mail address: dudsadee.utt@kmutt.ac.th (D. Uttapap).

0144-8617/$ – see front matter © 2013 Elsevier Ltd. All rights reserved.
http://dx.doi.org/10.1016/j.carbpol.2013.04.044

surface change/partial gelatinization was found on granules of rice starches. The crystallinity of starch samples, except waxy potato starch, decreased significantly with HMT. The treated starches (except waxy potato starch) had higher pasting temperature and lower viscosity. Shifts of the gelatinization temperature to higher values and gelatinization enthalpy to lower values, as well as biphasic endotherms, were found in treated starches (Jiranuntakul et al., 2011). The analysis of starch chain distribution and unit chain distribution of amylopectin revealed that HMT did not alter the molecular structure of starch and amylopectin (Jiranuntakul, Puttanlek, Rungsardthong, Puncha-arnon, & Uttapap, 2012). The significant decrease in paste viscosity and marked increase in gelatinization temperature, in spite of the decrease in crystallinity and gelatinization enthalpy of HMT starches, are still not well understood. Molecular changes as mentioned above might take part in the observed effects. However, starch granule structure is complex and consists of several levels of organization, i.e. granules, growth rings, blocklets, amorphous and crystalline lamellae, and amylopectin and amylose chains (Pérez & Bertoft, 2010; Vandeputte & Delcour, 2004); therefore, changes in other structural levels could also take place during HMT. Regarding the results obtained, we have speculated that a new superficial layer was formed on the surface of starch granules during HMT, and this layer restricted water penetration into the granules and retarded granule swelling. However, the proposed structure on the surface region of starch granules was not observed by scanning electron microscopy (SEM). This might be due to the fact that resolution of this technique was not high enough to examine the nano-structure of the starch granules. Gunning, Kirby, Morris, Wells, and Brooker (1995) reported that preparation of samples for imaging by coating with metals provided thin surface coats of around 10 nm thickness. Such coats are particulate, leading to the possible misinterpretation of results at very high resolution due to the presence and size of the metal grains. To overcome this problem, a new technique should be employed to explore the nanostructure of the starch granules.

Atomic force microscopy (AFM) is a powerful technique for investigating biological surfaces, such as food materials. This technique has a high magnification with high resolution for observing nanometer-scale structures, and a high capacity for imaging samples in either atmospheric or aqueous environments without any dyeing, metal coating, or fluorescence of samples; this allows the observation of the sample structure in its nearly native condition (Yang et al., 2007). This technique has been applied by several researchers to study the external and internal structures of starch granules (Ayoub, Ohtani, & Sugiyama, 2006; Baldwin, Adler, Davies, & Melia, 1998; Juszczak, Fortuna, & Krok, 2003a,b; Ohtani, Yoshino, Hagiwara, & Maekawa, 2000; Ridout, Parker, Hedley, Bogracheva, & Morris, 2004). Depressions and protrusions on the surface of potato, tapioca, barley, oat, maize, waxy maize, wheat, rye, and rice starch granules were also viewed by AFM operated in non-contact mode (Juszczak et al., 2003a,b). Ohtani et al. (2000) observed protrusions approximately 30 nm in diameter on the outermost surface of rice, corn, wheat, potato, and sweet potato starch granules, physically destroyed by a glass homogenizer. A significant change in the surface structure of rice starch granules, which was disordered using plasticizing combined with a lyophilization process, was detected by AFM. The average size of protrusions on the granule surface of rice starch decreased from 100 to 35 and 25 nm after the second and the third disorder processes, respectively (Ayoub et al., 2006).

In this study, AFM, operated in intermittent contact mode, was conducted to investigate changes of the surface structure of waxy and normal rice, corn, and potato starch granules after HMT at 100 °C for 16 h with a moisture content of 25%. AFM images of starch granules prior to and following HMT were examined and analyzed for the size of protrusions and the width and depth of existing pores or pits. Alterations of these surface characteristics were traced and compared among the starch samples. Associations of the surface changes with the crystalline structure and gelatinization properties of HMT starches were also discussed.

2. Materials and methods

2.1. Materials

Normal rice (Pathum Thani 60) and waxy rice (RD 6) were provided by the Pathum Thani Rice Research Center, Thanyaburi, Pathum Thani, Thailand. Normal corn (sweet type), waxy corn, and normal potatoes were purchased at a local market in Bangkok, Thailand. Waxy potato starch (3.92% amylose content) was provided by National Starch Food Innovation.

2.2. Starch isolation

Normal rice, waxy rice, normal corn, waxy corn, and normal potato starches, with amylose contents of 21.72%, 1.64%, 25.19%, 2.06%, and 28.97%, respectively, were isolated from their sources by the methods described by Jiranuntakul et al. (2011).

2.3. Heat–moisture treatment

Native starch was brought to the desired moisture content (25%) by soaking 200 g of starch in 600 mL of water overnight at 4 °C. Excess water in the equilibrated slurry was drawn out by vacuum suction to obtain a starch cake. The cake obtained was rendered into small lumps by pressing the cake through a sieve (mesh size 2.36 mm) onto a tray. Water in the starch lumps was then evaporated by open air-drying until the moisture content dropped to 25%. Starch samples with adjusted moisture content were placed in 200 mL screw-capped bottles and heated in a hot-air oven at 100 °C for 16 h. After HMT, the bottles were opened and the starches were dried at 40 °C until the moisture content reached 10%.

2.4. Sample preparation for AFM imaging

Immobilization of starch granules was performed before AFM imaging by the following procedure. Untreated or HMT starch granules (20 mg) were mixed with 1 mL of MilliQ water (Millipore, Billerica MA). Then 50 μL samples of starch suspensions were taken with a pipette and dropped onto a glass slide. Excess water was removed from the sample by heating at 40 °C for 30 min using a temperature controllable hot plate.

2.5. Atomic force microscopy

AFM images of untreated or HMT starches were obtained using an AFM (Nanowizard; JPK Instruments AG, Berlin, Germany) and a standard silicon tip cantilever (OMCL-AC160TS-C2; Olympus, Japan) with typical resonant frequency and spring constant of 300 kHz and 42 N/m, respectively. The measurements were performed in air at ambient temperature (25 °C) and humidity using intermittent contact mode (also called tapping mode). Scan areas varied between 500 nm × 500 nm and 40 μm × 40 μm, with scan frequency in the range of 0.1–1.0 Hz. For each starch sample, topographic and error signal mode images of approximately 40–50 starch granules were collected, and a typical representative sample was selected as an illustrative result. Bright regions in the AFM topographic images correspond to peak features in height. The error signal mode was used to enhance the edge contrast of the sample (Ohtani et al., 2000). JPK Image Processing software (JPK Instruments) was used for analysis of the AFM images.

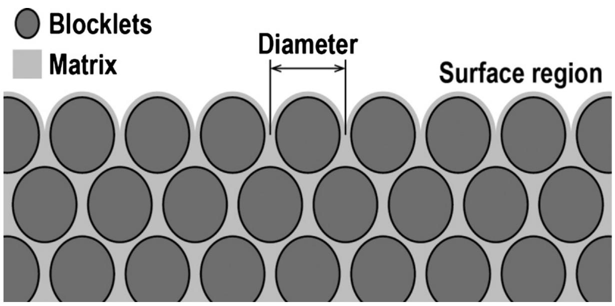

Fig. 1. Schematic diagram demonstrating the measurement of protrusion size on the surface region of a starch granule.

2.6. Measurement of protrusion size

For the measurement of protrusion sizes on the surface region of starch granules, 10 AFM topographic images were taken of different starch granules (scan size 1 μm × 1 μm). For each image, only certain protrusions were chosen to measure their diameter. The recorded data consisted of 30 protrusions per image, which resulted in a total number of 300 evaluated protrusions per starch sample. The protrusion size was denoted as "apparent diameter", which was defined as the width at the base of the protrusion (Fig. 1) using the Section tool in the image processing software.

2.7. Statistical analysis

The experimental data obtained from AFM images were analyzed using an independent samples *t*-test, and were expressed as mean value ± standard deviation. A Levene's test was conducted to examine significant differences between the experimental mean values for each pair of untreated and HMT starches ($p \leq 0.05$).

3. Results and discussion

Topographic and error signal mode AFM images of the surface region of untreated and HMT starch granules are shown in Figs. 2–5. The size variation of the protrusions on the surface of starch granules obtained from the AFM images are shown by histograms in Fig. 6. The corresponding average protrusion sizes, as well as the extents of the smooth surface region, are given in Table 1.

3.1. Untreated starch granules

AFM topographic and error signal mode images of the surface region of all untreated starch granules are shown in Fig. 2. The images revealed that the surfaces of all starch granules were rough and consisted of small protrusions. The degree of surface roughness increased from rice starch to corn and potato starches, respectively. When comparing normal and waxy types of starch from the same botanical source, it was found that normal and waxy rice starches displayed some different features. The surface of normal rice starch

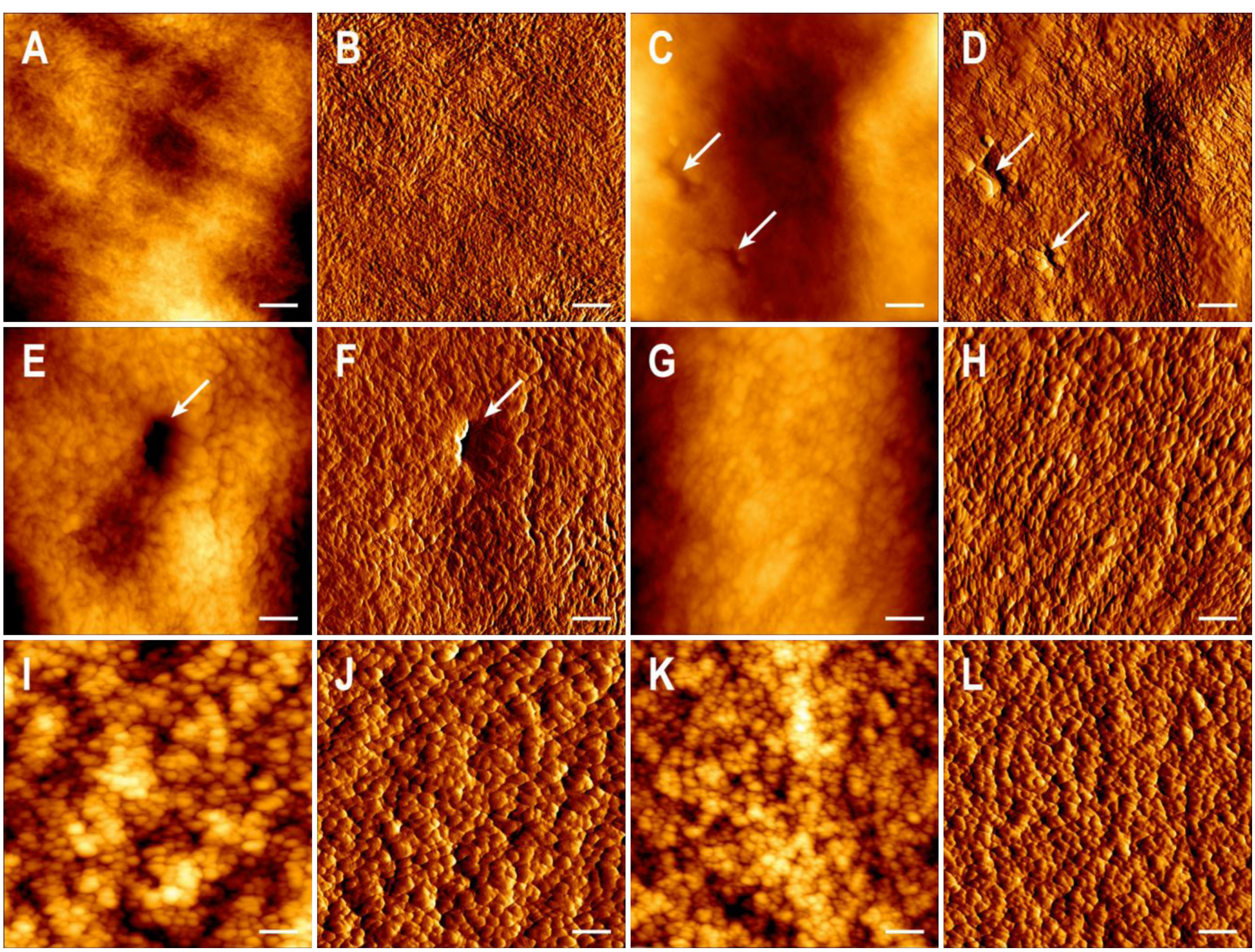

Fig. 2. AFM topographic (1st and 3rd column) and error signal mode (2nd and 4th column) images of the surface region of untreated starch granules: (A and B) normal rice, (C and D) waxy rice, (E and F) normal corn, (G and H) waxy corn, (I and J) normal potato, and (K and L) waxy potato. Scan size is 2 μm × 2 μm (bar = 250 nm).

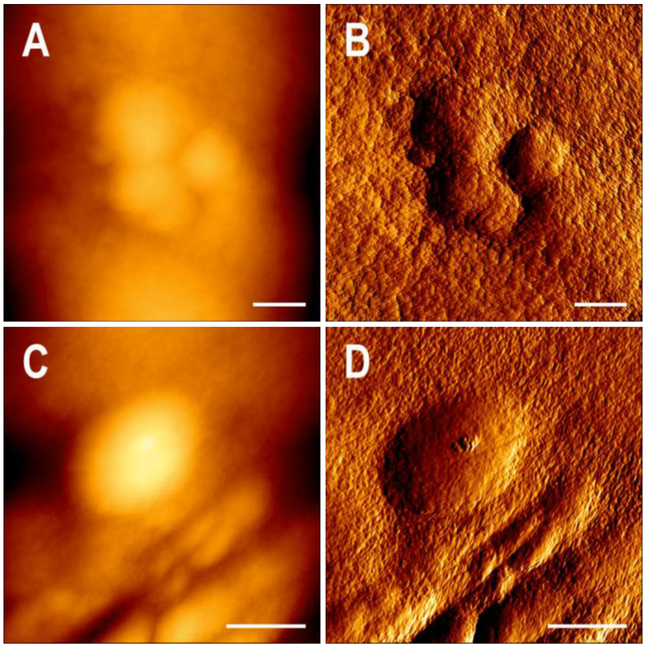

Fig. 3. AFM topographic (left column) and error signal mode (right column) images of the very rough surface region of untreated starch granules: (A and B) normal potato, and (C and D) waxy potato. Scan sizes are (A and B) 6 μm × 6 μm and (C and D) 4 μm × 4 μm (bar = 1 μm).

was more uniform than that of the waxy type. Scanning of the entire surface of normal rice granules revealed no distinct pores, while a few pits (≈200 nm) were observed on the surface of the waxy type. In addition, a smooth area of approximately 5–10% was found on the surface of waxy rice starch. The protrusion sizes of normal and waxy rice starches were estimated to be 28 and 27 nm, respectively (Table 1). The protrusions of corn starches were larger and displayed a clearer shape as compared to the rice starches. Most of the protrusions were oval-shaped. Pores of approximately 250 nm in size were found distributed over the surface of normal corn granules, whereas no such pores were observed on the surface of waxy-type granules. Protrusion sizes of the normal and waxy corn starches were 34 and 44 nm, respectively. On the other hand, the surfaces of normal and waxy-type potato starch granules were very similar to each other, i.e. each surface was homogeneous and no pores were found. Among the samples, normal potato starch displayed the largest protrusions (≈56 nm). Waxy-type potato starch granules contained some smaller protrusions, with an average size of ≈51 nm.

Protrusions on the surface of starch granules have been observed for rice (Ayoub et al., 2006; Juszczak et al., 2003b), corn (Juszczak et al., 2003b; Sujka & Jamroz, 2009), wheat (Baldwin et al., 1998), barley (Juszczak et al., 2003b), rye (Juszczak et al., 2003b), potato (Baldwin et al., 1998; Juszczak et al., 2003a; Sujka & Jamroz, 2009; Szymońska, Krok, Komorowska-Czepirska, & Rębilas, 2003), and tapioca (Juszczak et al., 2003a). Protrusions on the cleaved surface of rice, corn, and pea starch granules sectioned using a microtome

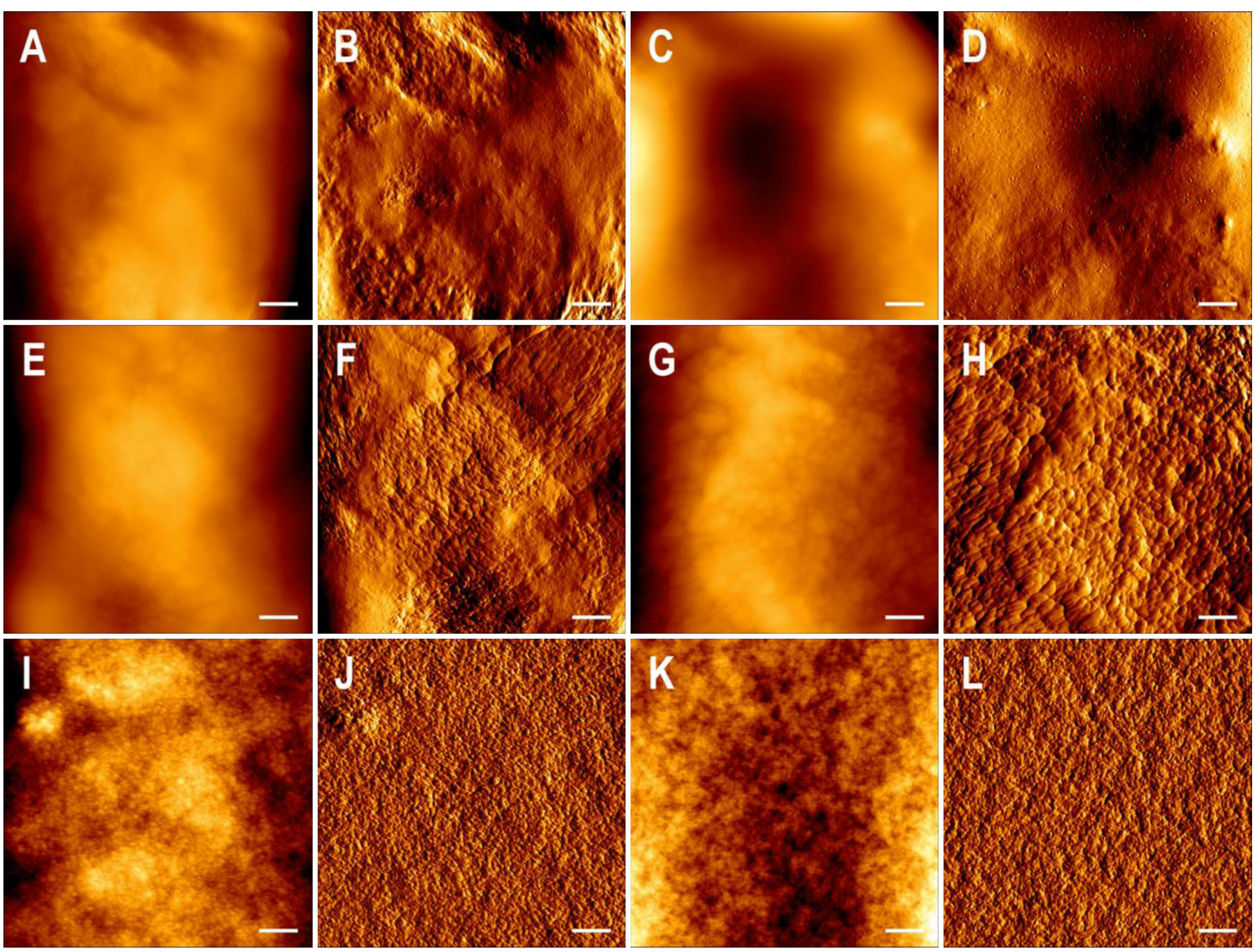

Fig. 4. AFM topographic (1st and 3rd column) and error signal mode (2nd and 4th column) images of the surface region of HMT starch granules: (A and B) normal rice, (C and D) waxy rice, (E and F) normal corn, (G and H) waxy corn, (I and J) normal potato, and (K and L) waxy potato. Scan size is 2 μm × 2 μm (bar = 250 nm).

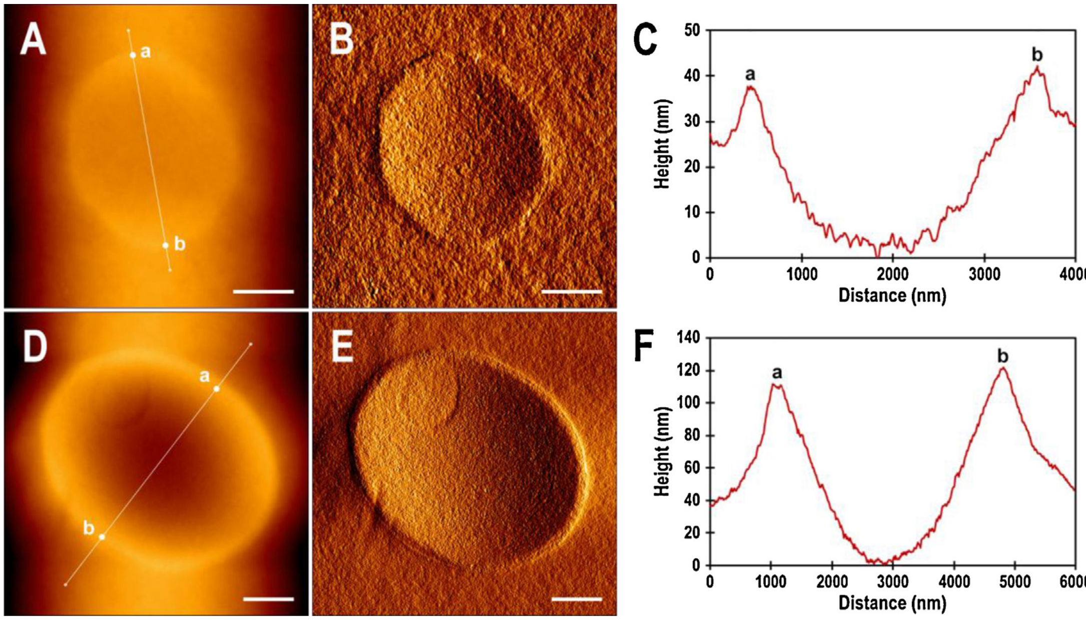

Fig. 5. AFM topographic image (left column), error signal mode image (middle column) and cross-section profile (right column) of the round-shaped depressions found on the surface region of HMT starch granules: (A–C) normal potato and (D–F) waxy potato. Scan sizes are (A and B) 5 μm × 5 μm and (C and D) 6 μm × 6 μm (bar = 1 μm). Heights in the cross-section profiles are the heights of the surface regions of starch granules in AFM topographic images (white line), with background data subtracted.

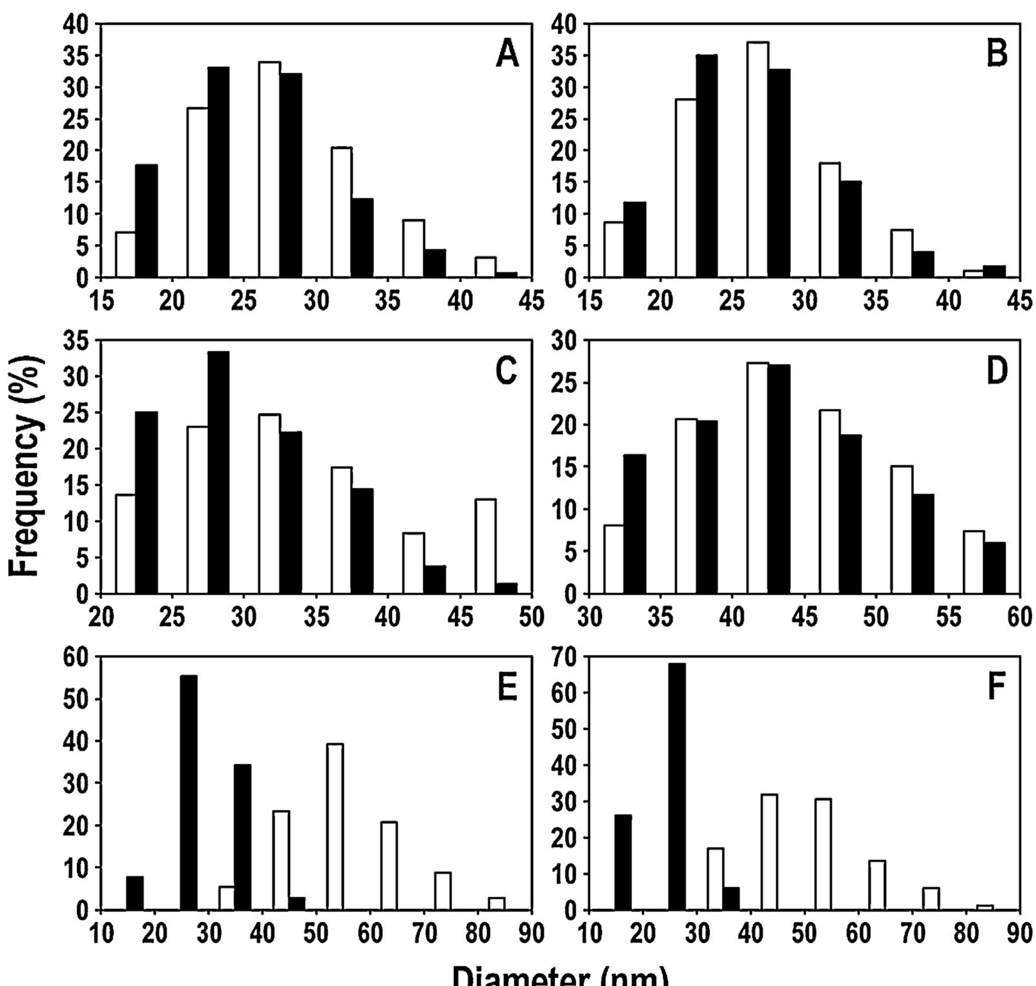

Fig. 6. Histograms showing the size variation of protrusions on the surface region of untreated and HMT starch granules obtained from analysis of AFM images: (A) normal rice, (B) waxy rice, (C) normal corn, (D) waxy corn, (E) normal potato, and (F) waxy potato. White and black bars represent the data from untreated and HMT starches, respectively.

Table 1
Average size of surface protrusions and the estimated extents of the smooth surface region of untreated and HMT starch granules.

Starch	Average size of protrusion (nm)[a,b]	Extent of surface covered with smooth regions[d]
Normal rice		
Untreated	27.87 ± 5.85[p]	–
HMT	25.10 ± 5.34[p]	+++
Waxy rice		
Untreated	26.96 ± 5.34	+
HMT	nd[c]	+++++
Normal corn		
Untreated	33.80 ± 8.38[p]	–
HMT	29.20 ± 6.26[p]	++
Waxy corn		
Untreated	44.27 ± 6.95[p]	–
HMT	42.61 ± 7.89[p]	+
Normal potato		
Untreated	56.02 ± 10.53[p]	–
HMT	28.29 ± 6.02[q]	–
Waxy potato		
Untreated	51.26 ± 10.80[p]	–
HMT	23.09 ± 4.51[q]	–

[a] Each value is express as mean ± standard deviations.
[b] Means with different letters in each pair of untreated and HMT starches are significantly different ($p \leq 0.05$).
[c] nd means not determined.
[d] Level of surface coverage with smooth regions qualitatively rated from no observed smooth region on surface of starch granules (−) to well-observed smooth region on surface of starch granules (+++++).

were also reported by Ohtani et al. (2000) and Ridout et al. (2004). This structure corresponds to the "blocklet", a term first used in 1937 by Badenhuizen to describe the association or clustering of amylopectin helices into effective spheres (Badenhuizen, 1937). However, the sizes of the blocklets reported by several researchers were different (Ayoub et al., 2006; Baldwin et al., 1998; Ohtani et al., 2000; Sujka & Jamroz, 2009). Gallant, Bouchet, and Baldwin (1997) described protrusions ranging between 20 and 500 nm in diameter, depending on the starch botanical type and location in the granule.

Unique topographies were found on the surface region of some starch granules. For waxy rice starch, some surface areas appeared smoother and had pits, as indicated by white arrows in Fig. 2C and D. The depth of the pits was approximately 25 nm. These observations indicated a defective structure of the surface region of the starch granules. AFM images also revealed that the surface of normal corn starch granules contains some pores, as indicated by white arrows in Fig. 2E and F. The length and depth of the observed pores were in the range of 200–325 nm and 60–100 nm, respectively. However, the measurement of the depth of pores on the surface may be inaccurate due to the limitations of the cantilever tip. Such pores were not observed on the surface area of waxy corn starch granules. Pores on the surface of corn starches have been reported by Juszczak et al. (2003b) and Sujka and Jamroz (2009). Sujka and Jamroz (2009) reported that the depth of these pores obtained from AFM profiles ranged between 41 and 68 nm.

In some surface regions of normal potato and waxy potato starch granules, bulges with approximate diameters of 1–2 μm were observed (Fig. 3). However, the area containing bulges was relatively small when compared with the total surface area. Very rough surface regions on potato starch granules, known as "blebs", have also been reported by Baldwin et al. (1998). Moreover, a scratch-like topography on some parts of normal and waxy potato starch surfaces was observed (figure not shown). The deepest points of the scratch-like structure were approximately 20–60 nm from the surface. This topography might occur by shear force, produced by pestle and mortar, acting on the surface of starch granules during the milling process in the starch isolation procedure. Although depressions on the granule surface of potato starches were not observed in our study, Juszczak et al. (2003a) found that depressions of about 0.4–1 μm in width were exhibited on the surface of potato starch.

3.2. HMT starch granules

AFM images of the surface region of HMT starch granules are presented in Figs. 4 and 5. The results show that the surface structure of normal and waxy starches was noticeably affected by HMT. Observed changes following HMT included the disappearance of some protrusions and pores, as well as the occurrence of smooth areas, small protrusions and round-shaped depressions. The extent of these transformations differed considerably among the starches (waxy rice > normal rice > normal corn > waxy corn > normal potato ≈ waxy potato). As shown in Fig. 4C and D, most of the surface of waxy rice granules was covered with a smooth area, and protrusions were rarely observed. For the normal type of rice granules, about half of the surface consisted of a smooth region, and the remaining protrusions were unclear (Fig. 4A and B). A lesser extent of the smooth region was found on the surface of normal corn starch, and the protrusion size appeared to be smaller as compared to the untreated starches (Fig. 4E and F); on the other hand, very limited changes were found on the surface of the waxy type (Fig. 4G and H). Changes of the surface structure of normal and waxy potato starches were comparable, i.e. protrusion sizes became obviously smaller; however, no (or very little) smooth regions were observed (Fig. 4I–L). In addition, some shallow, round-shaped depressions were found on the surface of HMT normal potato (Fig. 5A and B) and waxy potato (Fig. 5D and E) starch granules. The approximate depth and width of these topographical features ranged between 40–120 nm and 3–4 μm, respectively (Fig. 5C and F). These structural features might arise during HMT from pressure on the softened surface of the starch granules by adjacent starch granules having harder surfaces. These data indicated that the stability of the surface structure of starches against transformation by HMT depended on the botanical origins. Results of AFM image analysis (Table 1) revealed that there was no statistical difference in the average size of protrusions on the surface region of each pair of untreated and HMT normal rice, normal corn, and waxy corn starch granules ($p > 0.05$). On the other hand, a significant reduction in the average size of protrusions after HMT ($p \leq 0.05$) was noticeable for normal potato (from 56 to 28 nm) and waxy potato starches (from 51 to 23 nm).

The smooth region appearing on the surface of HMT rice and corn starch granules, as mentioned above, is thought to be caused by melting of the protrusions (referred to as "gelatinization" in starch chemistry). A schematic diagram representing this phenomenon is shown in Fig. 7A. [It is worth noting here that except for waxy rice starch, such a change could not be observed by scanning electron microscopy, as reported in our earlier work (Jiranuntakul et al., 2011).] Accordingly, we speculated that the developed structure would act as a barrier which restricted water penetration into starch granules and shifted gelatinization endotherms to the higher temperature (Jiranuntakul et al., 2011).

In the case of HMT potato starches, although the smooth region was not observed, the oval-shaped protrusions became smaller and their shapes were not as clear as those on untreated starches. These structural changes would also be associated with the limited swelling and increase of gelatinization temperature of potato starches after HMT, as reported by Jiranuntakul et al. (2011). We hypothesized that there were at least two phenomena participating in the morphological changes of protrusions on the surface of potato starch granules: (1) partial melting of the protrusions; and (2) compression of amylopectin double helix chains. Partial

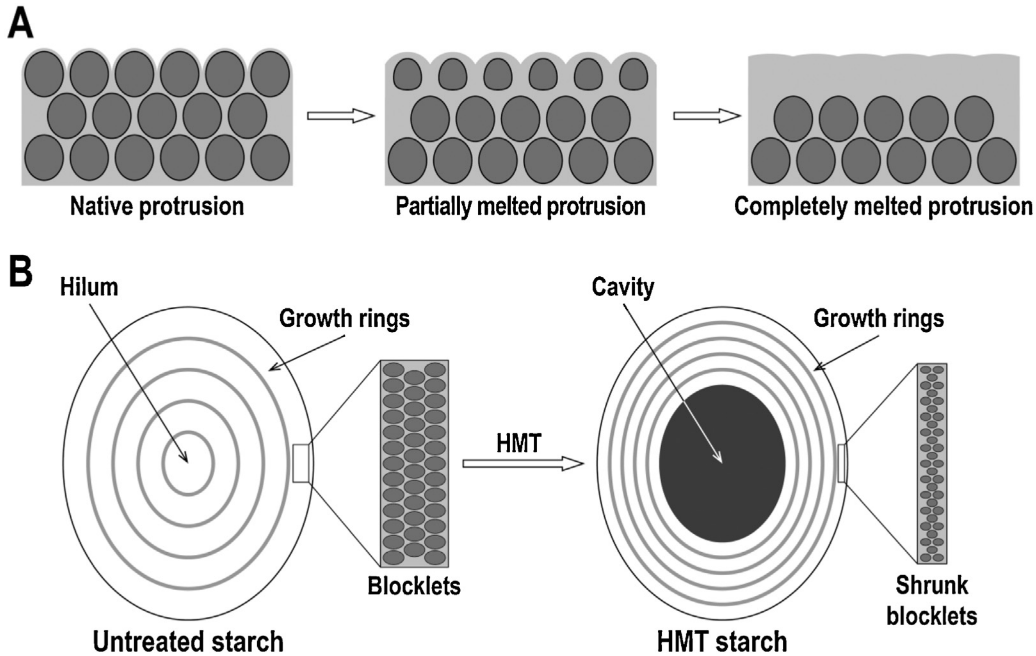

Fig. 7. Schematic diagram showing (A) the melting of protrusions on the surface region of a starch granule during HMT, and (B) the reduction in size of protrusions (blocklets) as well as the development of a cavity at the center of a HMT potato starch granule.

melting of the protrusions was more readily acceptable, as it was evidenced by the flatter granular surface and more irregular shape of protrusions after HMT (Fig. 7A). As shown in Fig. 7B, however, considering the crystalline structure of potato starch (B-type crystalline pattern), it is also possible that the reduced size of potato starch granule protrusions could be attributed to the more open packing of the helices of B-type starch, with 36–42 water molecules per unit cell (Imberty & Pérez, 1988). During HMT, the water molecules in these unit cells could evaporate and cause the amylopectin double helix chains to rearrange into a denser packing structure, resulting in the shrinkage of protrusions. This supposition was supported by the transformation of the crystalline pattern of potato starch from B- to A-type as a result of HMT (Jiranuntakul et al., 2011). Although the internal structure of starch granules was not examined in this study, hollow cavities or channels inside the starch granules that occur after HMT have been reported by several researchers (Kawabata et al., 1994; Lee, Kim, Choi, & Moon, 2012; Lee, Shin, Kim, Choi, & Moon, 2011; Vermeylen, Goderis, & Delcour, 2006). According to our proposed explanation, shrinkage of the protrusions may result in the development of a cavity. To verify this, the internal changes must be examined further.

Changes of the surface topography of starch granules after various treatments have been reported by several researchers. Szymońska et al. (2003) studied the influence of multiple deep-freezing and thawing on the surface of potato starch granules by AFM (non-contact mode). The authors demonstrated that a well-ordered structure of the surface, with distinct straight chains of protrusions of about 30 nm in diameter, could be observed after five repetitions of freezing in liquid nitrogen followed by thawing. The multiple freezing/thawing processes might cause disruption of the crystalline arrangement inside the starch granule and weakening of the interactions between the double helices. The surface characteristics of potato and corn starch granules after being hydrolyzed by *Bacillus subtilis* α-amylase were investigated by Sujka and Jamroz (2009). They found that the surface of the hydrolyzed granules was much rougher than that of native granules, and protrusions on the surface became more distinct.

4. Conclusions

In this study, changes in the surface topography of starch granules after HMT were evidenced by AFM. The disappearance of some protrusions and pores, as well as the development of smooth areas, small protrusions and round-shaped depressions, was observed to varying degrees on the surface region of rice, corn, and potato starch granules. These surface changes may to a certain extent be related to their crystalline structure and gelatinization properties. Further investigation of the internal structure of starch granules, as well as investigation of the other B-type starches, will help achieve a more complete understanding of the properties of HMT starch.

Acknowledgments

The authors would like to thank the Thailand Research Fund (TRF) for financial support via The Royal Golden Jubilee Ph.D. Program (RGJ) for Mr. Wittawat Jiranuntakul (part of the Ph.D. Program of King Mongkut's University of Technology Thonburi).

References

Ayoub, A., Ohtani, T., & Sugiyama, S. (2006). Atomic force microscopy investigation of disorder process on rice starch granule surface. *Starch/Stärke*, *58*, 475–479.
Badenhuizen, N. P. (1937). Die struktur des stärkekorns. *Protoplasma*, *28*, 293–326.
Baldwin, P. M., Adler, J., Davies, M. C., & Melia, C. D. (1998). High resolution imaging of starch granule surfaces by atomic force microscopy. *Journal of Cereal Science*, *27*, 255–265.
Chung, H. J., Hoover, R., & Liu, Q. (2009). The impact of single and dual hydrothermal modifications on the molecular structure and physicochemical properties of normal corn starch. *International Journal of Biological Macromolecules*, *44*, 203–210.
Gallant, D. J., Bouchet, B., & Baldwin, P. M. (1997). Microscopy of starch: Evidence of a new level of granule organization. *Carbohydrate Polymers*, *32*, 177–191.
Gunning, A. P., Kirby, A. R., Morris, V. J., Wells, B., & Brooker, B. E. (1995). Imaging bacterial polysaccharides by AFM. *Polymer Bulletin*, *34*, 615–619.
Hoover, R., & Manuel, H. (1996). The effect of heat–moisture treatment on the structure and physicochemical properties of normal maize, waxy maize, dull waxy maize and amylomaize V starches. *Journal of Cereal Science*, *23*, 153–162.
Hormdok, R., & Noomhorm, A. (2007). Hydrothermal treatments of rice starch for improvement of rice noodle quality. *LWT – Food Science and Technology*, *40*, 1723–1731.

Imberty, A., & Pérez, S. (1988). A revisit to the three-dimensional structure of B-type starch. *Biopolymers*, *27*, 1205–1221.

Jacobs, H., & Delcour, J. A. (1998). Hydrothermal modifications of granular starch, with retention of the granular structure: A review. *Journal of Agricultural and Food Chemistry*, *46*, 2895–2905.

Jiranuntakul, W., Puttanlek, C., Rungsardthong, V., Puncha-arnon, S., & Uttapap, D. (2011). Microstructural and physicochemical properties of heat–moisture treated waxy and normal starches. *Journal of Food Engineering*, *104*, 246–258.

Jiranuntakul, W., Puttanlek, C., Rungsardthong, V., Puncha-arnon, S., & Uttapap, D. (2012). Amylopectin structure of heat–moisture treated starches. *Starch/Stärke*, *64*, 470–480.

Juansang, J., Puttanlek, C., Rungsardthong, V., Puncha-Arnon, S., & Uttapap, D. (2012). Effect of gelatinisation on slowly digestible starch and resistant starch of heat–moisture treated and chemically modified canna starches. *Food Chemistry*, *131*, 500–507.

Juszczak, L., Fortuna, T., & Krok, F. (2003a). Non-contact atomic force microscopy of starch granules surface. Part I. Potato and tapioca starches. *Starch/Stärke*, *55*, 1–7.

Juszczak, L., Fortuna, T., & Krok, F. (2003b). Non-contact atomic force microscopy of starch granules surface. Part II. Selected cereal starches. *Starch/Stärke*, *55*, 8–16.

Kawabata, A., Takase, N., Miyoshi, E., Sawayama, S., Kimura, T., & Kudo, K. (1994). Microscopic observation and X-ray diffractometry of heat/moisture-treated starch granules. *Starch/Stärke*, *46*, 463–469.

Lee, C. J., Kim, Y., Choi, S. J., & Moon, T. W. (2012). Slowly digestible starch from heat–moisture treated waxy potato starch: Preparation, structural characteristics, and glucose response in mice. *Food Chemistry*, *133*, 1222–1229.

Lee, C. J., Shin, S. I., Kim, Y., Choi, H. J., & Moon, T. W. (2011). Structural characteristics and glucose response in mice of potato starch modified by hydrothermal treatments. *Carbohydrate Polymers*, *83*, 1879–1886.

Ohtani, T., Yoshino, T., Hagiwara, S., & Maekawa, T. (2000). High-resolution imaging of starch granule structure using atomic force microscopy. *Starch/Stärke*, *52*, 150–153.

Pérez, S., & Bertoft, E. (2010). The molecular structures of starch components and their contribution to the architecture of starch granules: A comprehensive review. *Starch/Stärke*, *62*, 389–420.

Ridout, M. J., Parker, M. L., Hedley, C. L., Bogracheva, T. Y., & Morris, V. J. (2004). Atomic force microscopy of pea starch: Origins of image contrast. *Biomacromolecules*, *5*, 1519–1527.

Shih, F., King, J., Daigle, K., An, H. J., & Ali, R. (2007). Physicochemical properties of rice starch modified by hydrothermal treatments. *Cereal Chemistry*, *84*, 527–531.

Singh, G. D., Bawa, A. S., Riar, C. S., & Saxena, D. C. (2009). Influence of heat–moisture treatment and acid modifications on physicochemical, rheological, thermal and morphological characteristics of Indian water chestnut (*Trapa natans*) starch and its application in biodegradable films. *Starch/Stärke*, *61*, 503–513.

Sujka, M., & Jamroz, J. (2009). α-Amylolysis of native potato and corn starches – SEM AFM, nitrogen and iodine sorption investigations. *LWT – Food Science and Technology*, *42*, 1219–1224.

Szymońska, J., Krok, F., Komorowska-Czepirska, E., & Rębilas, K. (2003). Modification of granular potato starch by multiple deep-freezing and thawing. *Carbohydrate Polymers*, *52*, 1–10.

Vandeputte, G. E., & Delcour, J. A. (2004). From sucrose to starch granule to starch physical behaviour: A focus on rice starch. *Carbohydrate Polymers*, *58*, 245–266.

Varatharajan, V., Hoover, R., Liu, Q., & Seetharaman, K. (2010). The impact of heat–moisture treatment on the molecular structure and physicochemical properties of normal and waxy potato starches. *Carbohydrate Polymers*, *81*, 466–475.

Vermeylen, R., Goderis, B., & Delcour, J. A. (2006). An X-ray study of hydrothermally treated potato starch. *Carbohydrate Polymers*, *64*, 364–375.

Vieira, F. C., & Sarmento, S. B. S. (2008). Heat–moisture treatment and enzymatic digestibility of Peruvian carrot, sweet potato and ginger starches. *Starch/Stärke*, *60*, 223–232.

Watcharatewinkul, Y., Puttanlek, C., Rungsardthong, V., & Uttapap, D. (2009). Pasting properties of a heat–moisture treated canna starch in relation to its structural characteristics. *Carbohydrate Polymers*, *75*, 505–511.

Watcharatewinkul, Y., Uttapap, D., Puttanlek, C., & Rungsardthong, V. (2010). Enzyme digestibility and acid/shear stability of heat–moisture treated canna starch. *Starch/Stärke*, *62*, 205–216.

Yang, H., Wang, Y., Lai, S., An, H., Li, Y., & Chen, F. (2007). Application of atomic force microscopy as a nanotechnology tool in food science. *Journal of Food Science*, *72*, R65–R75.

Zavareze, E. R., Storck, C. R., Castro, L. A. S., Schirmer, M. A., & Dias, A. R. G. (2010). Effect of heat–moisture treatment on rice starch of varying amylose content. *Food Chemistry*, *121*, 358–365.